Optimal Day-Ahead Scheduling for Active Distribution Network Considering Uncertainty

Kasi Vemalaiah[1], SIEEE, Dheeraj Kumar Khatod[1], MIEEE, Narayana Prasad Padhy[1,2,3], SMIEEE
[1]Electrical Engineering Department, Indian Institute of Technology Roorkee, Roorkee, India.
[2]Director, Malaviya National Institute of Technology Jaipur, Jaipur, Rajasthan, India.
[3]Mentor Director, Indian Institute of Information Technology Kota, Jaipur, Rajasthan, India.
Email: {kasi_v, dheeraj.khatod, nppadhy}@ee.iitr.ac.in.

2022 IEEE International Conference on Power Electronics, Drives and Energy Systems (PEDES) | 978-1-6654-5566-4/22/$31.00 ©2022 IEEE | DOI: 10.1109/PEDES56012.2022.10080135

***Abstract*—In recent days, the adoption of the battery energy storage system has increased in the electric grid due to the massive integration of renewable energy sources. This paper proposes a two-stage stochastic optimal day-ahead scheduling of an active distribution network considering uncertainty. It seeks to define an optimal day-ahead dispatch of battery energy storage systems and switchable capacitor banks to diminish operational costs incurred. The scheduling problem includes second-order cone programming power flow to capture distribution network features and assures the global optimal solution. The normal and beta probability distribution functions have been employed to model the forecast error uncertainty of load demand and generation from renewable resources, respectively. The Monte Carlo simulation approach is utilized to generate a large number of scenarios. Further, to make the proposed algorithm computationally efficient, these large number of scenarios are reduced to a small number using the Kantorovich probability distance approach ensuring problem tractability. The proposed framework is developed as a mixed-integer second-order cone programming problem, coded in GAMS, and solved with a GUROBI solver. The presented results on the modified IEEE 33-bus distribution network show reduced operating costs, reduced energy losses, decreased peak demand, and a notably enhanced voltage profile.**

***Index Terms*—Active distribution network, day-ahead scheduling, mixed-integer second-order cone program, scenario generation and reduction, two-stage stochastic programming.**

NOMENCLATURE

Indices

i, j	The bus index.
ij	The branch index.
t	The time interval index.

Sets

$\Phi/\Phi^{\mathrm{LD}}/\Phi^{\mathrm{UG}}$	Set of network/load/upper grid buses.
$\Phi^{\mathrm{BESS}}/\Phi^{\mathrm{SCB}}$	Set of buses coupled with BESS/SCB.
$\Phi^{\mathrm{PV}}/\Phi^{\mathrm{WT}}$	Set of buses coupled with PV/WT.
T	Set of time intervals.

Parameters

$\eta_i^{\mathrm{ch}}/\eta_i^{\mathrm{dis}}$	Charging/discharging efficiency of i^{th} BESS.
$C^{\mathrm{BESS}}/C^{\mathrm{SCB}}$	Operational cost of i^{th} BESS/SCB.
$C_t^{\mathrm{UG}}/k_q^{\mathrm{UG}}$	Upper grid active power purchase price and its reactive counter part.
$E_{i,min}^{\mathrm{BESS}}/E_{i,max}^{\mathrm{BESS}}$	Minimum/maximum energy capacity limits of i^{th} BESS.
$I_{ij,max}$	Maximum current carrying capacity of ij^{th} line.
$N_{i,max}^{\mathrm{SCB}}/Y_{i,max}^{\mathrm{SCB}}$	Maximum permissible switching actions in a day/Maximum banks of i^{th} SCB.
$P_{i,min}^{\mathrm{UG}}/P_{i,max}^{\mathrm{UG}}$	Minimum/maximum active power limits of upper grid.
$P_{ij,max}/Q_{ij,max}$	Active/Reactive power capacity limits of ij^{th} line.
$Q_{i,min}^{\mathrm{UG}}/Q_{i,max}^{\mathrm{UG}}$	Minimum/maximum reactive power limits of upper grid.
$Q_{i,step}^{\mathrm{SCB}}$	Step size of i^{th} SCB.
$S_{i,max}^{\mathrm{BESS}}$	The i^{th} BESS peak apparent power.
$V_{i,max}/V_{i,min}$	Voltage maximum/minimum bounds of i^{th} bus.

Variables

$\gamma_{i,t}^{\mathrm{ch}}/\gamma_{i,t}^{\mathrm{dis}}$	Binary variables corresponding to charge/discharge position of i^{th} BESS.
$P_{i,t}^{\mathrm{ch}}/P_{i,t}^{\mathrm{dis}}$	Continuous variables corresponding to charge/discharge active power of i^{th} BESS.
$Q_{i,t}^{\mathrm{BESS}}/E_{i,t}^{\mathrm{BESS}}$	Continuous variables corresponding to reactive power/energy state of i^{th} BESS.
$\gamma_{i,t}^{\mathrm{SCB,UP}}/\gamma_{i,t}^{\mathrm{SCB,DN}}$	Binary variables corresponding to up/down regulation status of i^{th} SCB.
$\rho_{i,t}^{\mathrm{SCB}}$	Integer variable corresponding to step status of i^{th} SCB.
$Q_{i,t}^{\mathrm{SCB}}$	Continuous variable corresponding reactive power of i^{th} SCB.
$P_{i,t}^{\mathrm{UG}}/Q_{i,t}^{\mathrm{UG}}$	Active/reactive powers of upper grid(sub-station).
$V_{i,t}/\theta_{i,t}$	Continuous variables corresponding to voltage magnitude and angle of i^{th} bus.
$P_{ij,t}/Q_{ij,t}$	Continuous variables corresponding to active/reactive power ij^{th} line.
$U_{i,t}/W_{ij,t}^{\mathrm{R}}/W_{ij,t}^{\mathrm{I}}$	New defined continuous variables corresponding to conic reformulation.

This work was supported by the Department of Science and Technology (DST) India Smart Grid Research initiative under the research grant "Indo–Danish collaboration for data-driven control and optimization for a highly Efficient Distribution Grid (ID-EDGe: DST-1390-EED)" project.

I. INTRODUCTION

The integration of active elements, such as, distributed generation, battery energy storage system (BESS), capacitor

978-1-6654-5566-4/22/$31.00 ©2022 IEEE

bank, etc. into existing electricity network is transforming it to an active distribution network (ADN). Though the integration of active elements offers a number of benefits such as peak shaving, reduction in the renewable energy curtailment, loss reduction, voltage profile improvement, energy arbitrage, etc. to the utility [1], [2], it also complicates the operation of ADN. Therefore, optimal operation of ADN in presence of active elements is being paid significant attention now-a-days.

A nonlinear programming framework based combined active-reactive optimal power flow in a distribution network with wind turbine (WT) generation and storage is discussed in [3]. In this work, the main objective is to reduce the costs of energy losses and wind power curtailment. A multi-objective problem formulation is developed in [4], [5] to set the dispatch of BESS and plug-in hybrid electric vehicles to improve the benefit of the distribution system. A two-stage scheduling scheme is proposed in [6] for the unbalanced distribution network, the first stage targets to look for a suitable unbalance index, and the second stage aims to minimize operational cost. A day-ahead optimal dispatch for the ADN, including BESS, is proposed in [7] to find optimal active-reactive dispatch from BESS. A Mutation-Improved Grey Wolf Optimizer is discussed in [8] to determine the optimal BESS scheduling with an aim to diminish the losses of ADN. For efficiently managing the urban microgrid, a day-ahead optimal power flow model is proposed in [9]. The works presented in [3]-[9] do not guarantee the global optimum due to non-convex formulation [3] and use of meta heuristic algorithms to solve the problem [4]- [9].

A mixed-integer second-order cone program (MISOCP) based scheduling of ADN is proposed in [10] to ensure the global optimum solution. Two convex relaxations based frameworks, i.e., the second-order cone programming and the semi-definite programming, are proposed in [11] to find out the optimal dispatch of BESS to minimize the losses and cost. However, in [3]- [11], the uncertainty associated with generation from renewable energy resources, and load are not accounted for in the scheduling framework. A coordinated multi-timescale dispatch is presented in [12] to control the on-load tap changer, capacitor bank, and inverter of renewable energy source (RES). However the effect of BESS integration into distribution system is not explored in this work.

To address the aforementioned gaps, this paper proposes a two-stage day-ahead scheduling of switchable capacitor bank (SCB) and BESS present in ADN. The objective is to minimize the operation and maintenance costs of BESS and SCB considering the uncertainty associated with load and generation from photovoltaic (PV) and WT based units. The problem is formulated as a MISOCP problem, ensuring the exact solution. A large number of scenarios are constructed employing the Monte Carlo simulation (MCS) technique. Thereupon, a fast forward selection framework based on the Kantorovich distance approach is applied to decrease the number of scenarios. The proposed formulation is applied on the modified IEEE 33-bus distribution network.

The remainder of this paper is organized as follows: The proposed scheduling concept is illustrated in Section II. Section III discusses uncertainty modeling and the stochastic variant of the day-ahead scheduling scheme. The specifications of the test system and the corresponding results are presented in section IV. Section V concludes the work presented in this paper.

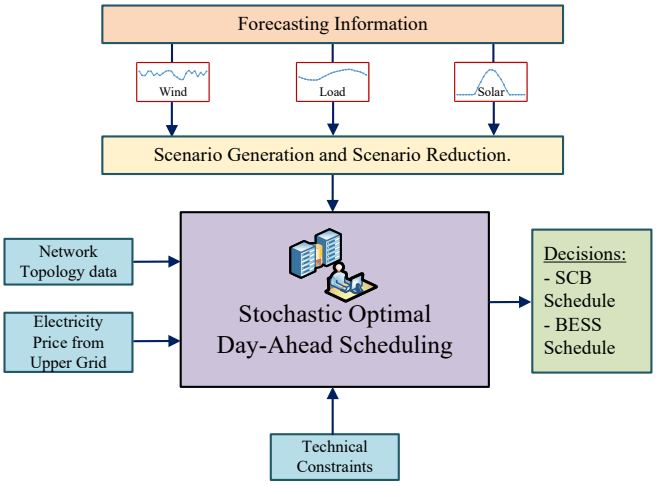

Fig. 1. Schematic diagram of proposed scheduling framework.

II. Proposed Day-Ahead Scheduling

The proposed day-ahead scheduling (DAS) framework aims to establish the optimum dispatch of BESS and SCB while taking into consideration all technological constraints. Fig. 1 illustrates the overall concept of the proposed DAS for ADN. DAS uses the forecast of load and generation (from PV and WT) as the primary input. Other than forecast of load and generation, DAS also considers the network topology, electricity price data from the upper grid and various technical and operational constraints. The results of DAS are communicated to BESSs and SCBs through their respective remote terminal units. By this way, the optimal decisions to maintain safe and efficient operation of ADN are taken.

A. Deterministic Day-Ahead Scheduling

This section presents the mathematical formulations for the deterministic DAS. In deterministic DAS framework, all forecasts are assumed to be accurate.

1) Objective Function:

$$\left.\begin{aligned}\min F = &\sum_{i\in\Phi^{\mathrm{UG}}}\sum_{t\in T}\left[C_t^{\mathrm{UG}}\,\Delta t\left(P_{i,t}^{\mathrm{UG}}+k_q^{\mathrm{UG}}Q_{i,t}^{\mathrm{UG}}\right)\right]+\\ &\sum_{i\in\Phi^{\mathrm{BESS}}}\sum_{t\in T}\left[\Delta t\,C^{\mathrm{BESS}}\left(P_{i,t}^{\mathrm{dis}}+P_{i,t}^{\mathrm{ch}}\right)\right]+\\ &\sum_{i\in\Phi^{\mathrm{SCB}}}\sum_{t\in T}\left[C^{\mathrm{SCB}}\left(\gamma_{i,t}^{\mathrm{SCB,UP}}+\gamma_{i,t}^{\mathrm{SCB,DN}}\right)\right]\end{aligned}\right\} \quad (1)$$

The objective function F seeks to minimize the day-ahead operational cost of the ADN. The first part in F represents the cost of energy procured from the upper grid through sub-station. The second and third parts in F represent the

operation and maintenance costs associated with BESS and SCB, respectively.

2) Constraints:

a) Battery Energy Storage System

$$\gamma_{i,t}^{\mathrm{ch}} + \gamma_{i,t}^{\mathrm{dis}} \leq 1,\ \forall t, \forall i \in \Phi^{\mathrm{BESS}} \tag{2}$$

$$\left.\begin{aligned} 0 \leq P_{i,t}^{\mathrm{ch}} \leq \gamma_{i,t}^{\mathrm{ch}} S_{i,max}^{\mathrm{BESS}} \\ 0 \leq P_{i,t}^{\mathrm{dis}} \leq \gamma_{i,t}^{\mathrm{dis}} S_{i,max}^{\mathrm{BESS}} \end{aligned}\right\} \forall t, \forall i \in \Phi^{\mathrm{BESS}} \tag{3}$$

$$\left.\begin{aligned} (P_{i,t}^{\mathrm{ch}})^2 + (Q_{i,t}^{\mathrm{BESS}})^2 \leq (S_{i,max}^{\mathrm{BESS}})^2 \\ (P_{i,t}^{\mathrm{dis}})^2 + (Q_{i,t}^{\mathrm{BESS}})^2 \leq (S_{i,max}^{\mathrm{BESS}})^2 \end{aligned}\right\} \forall t, \forall i \in \Phi^{\mathrm{BESS}} \tag{4}$$

$$\left.\begin{aligned} E_{i,t+1}^{\mathrm{BESS}} = E_{i,t}^{\mathrm{BESS}} + \Delta t\, \eta_i^{\mathrm{ch}} P_{i,t}^{\mathrm{ch}} - \Delta t\, \eta_i^{\mathrm{dis}} P_{i,t}^{\mathrm{dis}} \\ E_{i,min}^{\mathrm{BESS}} \leq E_{i,t}^{\mathrm{BESS}} \leq E_{i,max}^{\mathrm{BESS}} \end{aligned}\right\} \forall t, \forall i \in \Phi^{\mathrm{BESS}} \tag{5}$$

Equation (2) regulates the BESSs to either charge or discharge during time interval t. The operating limitations for the active power of BESSs is described in (3). Equation (4) represents the convex quadratic constraints associated with active and reactive power injections from BESSs. Energy state of BESSs at every time interval t, as well as the limitations on the energy of BESSs are given in (5).

b) Switchable Capacitor Bank

$$\gamma_{i,t}^{\mathrm{SCB,UP}} + \gamma_{i,t}^{\mathrm{SCB,DN}} \leq 1,\ \forall t, \forall i \in \Phi^{\mathrm{SCB}} \tag{6}$$

$$\sum_{t \in T} \left(\gamma_{i,t}^{\mathrm{SCB,UP}} + \gamma_{i,t}^{\mathrm{SCB,DN}}\right) \leq N_{i,max}^{\mathrm{SCB}},\ \forall i \in \Phi^{\mathrm{SCB}} \tag{7}$$

$$\left.\begin{aligned} \rho_{i,t}^{\mathrm{SCB}} - \rho_{i,t-1}^{\mathrm{SCB}} \leq \gamma_{i,t}^{\mathrm{SCB,UP}} Y_{i,max}^{\mathrm{SCB}} - \gamma_{i,t}^{\mathrm{SCB,DN}} \\ \rho_{i,t}^{\mathrm{SCB}} - \rho_{i,t-1}^{\mathrm{SCB}} \geq \gamma_{j,t}^{\mathrm{SCB,UP}} - \gamma_{i,t}^{\mathrm{SCB,DN}} Y_{i,max}^{\mathrm{SCB}} \end{aligned}\right\} \forall t, \forall i \in \Phi^{\mathrm{SCB}} \tag{8}$$

$$Q_{i,t}^{\mathrm{SCB}} = \rho_{i,t}^{\mathrm{SCB}} \cdot Q_{i,step}^{\mathrm{SCB}},\ \forall t,\ \forall i \in \Phi^{\mathrm{SCB}} \tag{9}$$

Equation (6) regulates the SCBs to either increase or decrease reactive power compensation during time interval t. Equation (7) restricts total switching actions of SCBs over a day to be within a maximum permissible value. After accounting for switching variables and total bank numbers, (8) limits the regulation span of SCBs. Equation (9) indicates the total reactive power injection from each SCB.

c) Power Flow Expressions

SOCP based power flow model, which can guarantee the exact solution, was proposed in [14]. The definition of new variables and expressions related to SOCP are

$$U_{i,t} = V_{i,t}^2/\sqrt{2}, \forall t, \forall i \in \Phi \tag{10}$$

$$\begin{aligned} W_{ij,t}^{\mathrm{R}} &= V_{i,t} V_{j,t} \cos(\theta_{i,t} - \theta_{j,t}) \\ W_{ij,t}^{\mathrm{I}} &= V_{i,t} V_{j,t} \sin(\theta_{i,t} - \theta_{j,t}), \forall t, \forall ij \end{aligned} \tag{11}$$

$$2U_{i,t}U_{j,t} \geq (W_{ij,t}^{\mathrm{R}})^2 + (W_{ij,t}^{\mathrm{I}})^2,\ \forall t, \forall ij \tag{12}$$

Expression (10) shows the conic constraint. These SOCP relaxations lead to global optimum, if (11) is exact [15]. For radial distribution system, (12) has been proven to be always exact [15]. The linear active & reactive powers flows of line ij at time interval t is given below

$$\left.\begin{aligned} P_{ij,t,s} = \sqrt{2} G_{ij} U_{i,t,s} - G_{ij} W_{ij,t,s}^{\mathrm{R}} - B_{ij} W_{ij,t,s}^{\mathrm{I}} \\ Q_{ij,t,s} = -\sqrt{2} B_{ij} U_{i,t,s} + B_{ij} W_{ij,t,s}^{\mathrm{R}} - G_{ij} W_{ij,t,s}^{\mathrm{I}} \end{aligned}\right\} \forall t, \forall ij \tag{13}$$

The bounds of power flow variables are as follows

$$\begin{aligned} &U_{i,t} = 1/\sqrt{2},\ \forall t, \forall i \in \Phi^{\mathrm{UG}} \\ &V_{i,min}^2/\sqrt{2} \leq U_{i,t} \leq V_{i,max}^2/\sqrt{2},\ \forall t, \forall i \in \Phi^{\mathrm{LD}} \end{aligned} \tag{14}$$

$$\left.\begin{aligned} -V_{i,max} V_{j,max} \leq W_{ij,t,s}^{\mathrm{I}} \leq V_{i,max} V_{j,max} \\ 0 \leq W_{ij,t,s}^{\mathrm{R}} \leq V_{i,max} V_{j,max} \end{aligned}\right\} \forall t, \forall ij \tag{15}$$

$$\left.\begin{aligned} -P_{ij,max} \leq P_{ij,t} \leq P_{ij,max} \\ -Q_{ij,max} \leq Q_{ij,t} \leq Q_{ij,max} \end{aligned}\right\} \forall t, \forall ij \tag{16}$$

The nodal power balance of the distribution network is given in the following equations

$$\left.\begin{aligned} P_{i,t}^{\mathrm{UG}} + \left(P_{i,t}^{\mathrm{dis}} - P_{i,t}^{\mathrm{ch}}\right) + P_{i,t}^{\mathrm{WT}} + P_{i,t}^{\mathrm{PV}} - P_{i,t}^{\mathrm{LD}} \\ = \sum_{j \in \Phi(i)} P_{ij,t} \\ Q_{i,t}^{\mathrm{UG}} + Q_{i,t}^{\mathrm{BESS}} + Q_{i,t}^{\mathrm{SCB}} - Q_{i,t}^{\mathrm{LD}} = \sum_{j \in \Phi(i)} Q_{ij,t} \end{aligned}\right\} \forall t, \forall i \tag{17}$$

Square of line current limit ($I_{ij,t}$) can be represented in the linear form as given below

$$\begin{aligned} I_{ij,t}^2 &= \sqrt{2}(G_{ij}^2 + B_{ij}^2)(U_{i,t} + U_{j,t} - 2W_{ij,t}^{\mathrm{R}}) \\ &\leq I_{ij,max}^2,\ \forall t, \forall ij \end{aligned} \tag{18}$$

Equations (1)-(9), (12)-(18) represent the MISOCP based deterministic day-ahead scheduling scheme.

B. Stochastic Day-Ahead Scheduling

This section presents the mathematical formulations for the stochastic DAS scheme. In stochastic DAS framework, all forecasts are considered to be uncertain. Therefore, first, the modelling of uncertainty from renewable generation (PV and WT) and load demand is presented in this section. Then, formulation of two-stage stochastic programming considering the uncertainty is presented in this section.

1) Modelling of Uncertainty: This subsection explains the modeling of forecasting error uncertainty associated with the PV generation, WT generation, and load. The forecast of load, and generation from PV and WT can be obtained by some of the classical regression techniques or data-driven machine learning algorithms, which is beyond the scope of this paper. The uncertainty of forecast generation of both PV and WT is assumed to follow the beta distribution function [12]. The beta distribution function is represented by the shape parameters α and β. urther, for each time interval, two Beta functions are used to model the predication errors: one for WT and the other for PV. The beta distribution function of forecasted generation, $P_{i,t}^{g,fore}$ is as follows

$$f_{P_{i,t}^{g,fore}}(x) = \frac{\Gamma(\alpha_{i,t} + \beta_{i,t})}{\Gamma(\alpha_{i,t})\Gamma(\beta_{i,t})}\, x^{\alpha_{i,t}-1}(1-x)^{\beta_{i,t}-1} \tag{19}$$

$$\sigma_{i,t}^{g} = 0.2\left[P_{i,t}^{g,fore}/P_i^{cap}\right] + 0.21 \tag{20}$$

$$\text{mean}: \left[P_{i,t}^{g,fore}/P_i^{cap}\right] = \alpha_{i,t}/[\alpha_{i,t}+\beta_{i,t}] \tag{21}$$

$$\text{variance}: (\sigma_{i,t}^{g})^2 = \frac{\alpha_{i,t}\beta_{i,t}}{(\alpha_{i,t}+\beta_{i,t})^2(\alpha_{i,t}+\beta_{i,t}+1)} \tag{22}$$

P_i^{cap} represents the capacity of i^{th} generating plant. Standard deviation of the predicted generation from PV and WT can be estimated by (20). Equations (21) and (22) define the relationship between shape parameters and mean and variance. One can estimate the shape parameters once the forecast of PV/WT generation is available. The shape parameters after solving (21) & (22) are given below

$$\alpha_{i,t} = \frac{P_i^{cap}(P_{i,t}^{g,fore})^2 - (P_{i,t}^{g,fore})^3}{(P_i^{cap})^3(\sigma_{i,t}^{g})^2} - \frac{P_{i,t}^{g,fore}}{P_i^{cap}} \tag{23}$$

$$\beta_{i,t} = \left[(P_i^{cap}/P_{i,t}^{g,fore}) - 1\right]\alpha_{i,t}, \tag{24}$$

The shape parameters of beta distribution function for both PV and WT for each time interval will be different due to non-identical values of standard deviation. Normal distribution function is used to represent load demand uncertainty with forecast value as the mean. To reflect the uncertainty in a decision making process, a large number of scenarios are necessary. For this purpose, MCS is utilized considering the probability distributions of forecast values. It is worth to mention here that as the number of scenarios is increased, the dimension of scheduling model also increases drastically, and hence, the available tools/solvers fail to converge in most of the cases. If the number of scenarios is reduced, the uncertainty in forecast variables is not well captured in the model, and hence, the realistic solution cannot be achieved. Therefore, the Kantorovich probability distance scenario reduction approach, which is based on fast forward selection framework [13], is used to reduce the number of scenarios. This ensures a good resemblance of the model uncertainty as well as computational tractability.

2) Two-Stage Stochastic Programming: This subsection presents the formulation of scheduling scheme which is framed as a two-stage stochastic problem [12] as given in (25). First stage objective in (25), $f(x)$ is the costs associated with BESS and SCB and the corresponding variables are the day-ahead dispatches of the BESS and SCB, respectively, which must not change during the real time operation i.e, before identifying the stochastic process's actual realization. Second stage objective in (25), $g(y)$ is the expected cost and include all variables associated with power flow, which can vary in the real time i.e., after identifying the stochastic process's actual realization. With finite number of scenarios $1, 2, ..., Ns$ having corresponding probabilities $\pi_1, ..., \pi_{Ns}$, respectively, the expectation expression in (25) can be replaced by (27).

$$\min_{x\in X}\{f(x) + E[Q(x,\sigma)]\} \tag{25}$$

$$Q(x,\sigma) = \min_{y\in\Omega(x,\sigma)} g(y) \tag{26}$$

$$E[Q(x,\sigma)] = \sum_{s=1}^{Ns}\pi_s E[Q(x,\sigma_s)] \tag{27}$$

TABLE I
DETAILS OF DIFFERENT ELEMENTS IN 33-BUS SYSTEM

Type	Location	Details of each element
PV	8, 20, 25, 30.	Rating = 0.6 MW.
WT	18, 33.	Rating = 0.6 MW.
SCB	6, 14, 17, 21, 24, 28.	$Q_{i,step}^{\text{SCB}} = 0.05$ MVAr, $\Psi_{i,max}^{\text{SCB}} = 5$, $N_{i,max}^{\text{SCB}} = 5, C_i^{\text{SCB}} = 0.5\$$.
BESS	12, 32.	$S_{i,max}^{\text{BS}} = 0.4$ MVA, $E_{i,max}^{\text{BS}} = 1.8$ MWh, $E_{i,min}^{\text{BS}} = 0.1$ MWh, $\eta_i^{\text{CH}} = 1/\eta_i^{\text{DIS}} = 0.9, C_i^{\text{BS}} = 5\$$/MW.
Other	-	$k_q^{UG} = 0.05$, $P_{ij,max}$ =5 pu, $I_{ij,max}$ = 5 pu, $V_{i,min} = 0.9$ pu, $V_{i,max} = 1.1$pu.

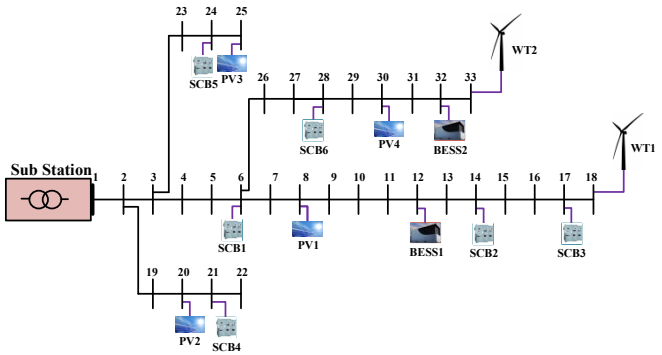

Fig. 2. Modified IEEE 33-bus active distribution network.

Two-stage stochastic framework can be represented in its deterministic equivalent form [12] as given in (28). The equivalent deterministic variant of the two-stage stochastic problem (28) is linear and can be combined with the MISOCP-based DAS scheme defined in section II-A.

$$\begin{aligned} &\min_{x,y_1,\ldots,y_{Ns}} f(x) + \sum_{s=1}^{Ns}\pi_s g(y_s) \\ &s.t. \quad x \in X;\ \ y_s \in \Omega(x,\sigma),\ \forall s \end{aligned} \tag{28}$$

The first and second stage variable sets in the proposed DAS scheme are given below.

$$x = \left[P_{i,t}^{\text{ch}}, P_{i,t}^{\text{dis}}, \gamma_{i,t}^{\text{ch}}, \gamma_{i,t}^{\text{dis}}, Q_{i,t}^{\text{BESS}}, E_{i,t}^{\text{BESS}}, \rho_{i,t}^{\text{SCB}}, Q_{i,t}^{\text{SCB}}, \gamma_{i,t}^{\text{SCB,UP}}, \gamma_{i,t}^{\text{SCB,DN}}\right]$$

$$y_s = \left[U_{i,t,s}, W_{ij,t,s}^{\text{R}}, W_{ij,t,s}^{\text{I}}, P_{ij,t,s}, Q_{ij,t,s}, P_{i,t,s}^{\text{UG}}, Q_{i,t,s}^{\text{UG}}\right]$$

III. CASE STUDY

This section presents simulation experiments conducted to examine the efficacy of the proposed two-stage stochastic DAS algorithm. The scheduling scheme is coded in GAMS software and solved with GUROBI solver. All the simulation experiments are carried out on an i7, 3.2 GHz and 16 GB RAM personal computer.

A. Specifications of Test System

A modified IEEE 33-bus system used for the validation of proposed scheduling is shown in Fig. 2. A modified IEEE 33-bus system is used for the validation of proposed DAS.

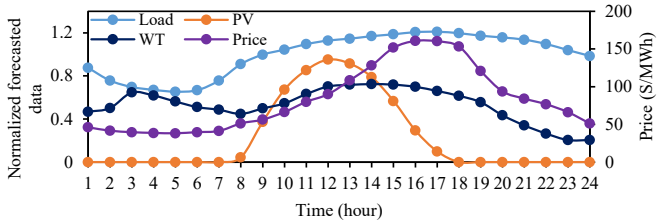

Fig. 3. Normalized forecasted information of load, PV generation, WT generation and the price from upper grid.

TABLE II
INFORMATION OF DIFFERENT CASES

Case	PV & WT	SCB	BESS	Uncertainty
C1	✓	X	X	X
C2	✓	✓	✓	X
C3	✓	X	X	✓
C4	✓	✓	✓	✓

The necessary data is obtained from [12]. The details of different elements connected to IEEE 33-bus are presented in Table I. The minimum and maximum limits of upper grid active/reactive power are 0 and 5 pu, respectively. The normalized forecast data corresponding to PV generation, WT generation, load demand, and upper grid price [16], [17] is shown in Fig. 3.

B. Results

The information regarding different cases is mentioned in Table II.

Case-1 (C1): It represents a normal deterministic operation of ADN without BESS and SCB. There is no forecast error present in this case. The corresponding apparent power intake and minimum voltage in the system are shown in Fig. 4.

Case-2 (C2): It represents the optimal deterministic scheduling of ADN coupled with BESS and SCB. There is no forecast error present in this case also. Fig. 5 depicts the system's apparent power intake and minimum voltage. The optimal charge/discharge power and energy state of both BESSs are shown in Fig.6(a). It is observed that both BESSs charge by receiving active power from the upper grid, when upper grid prices are low and discharge by delivering active power to the upper grid, when upper grid prices are high. Similarly, the

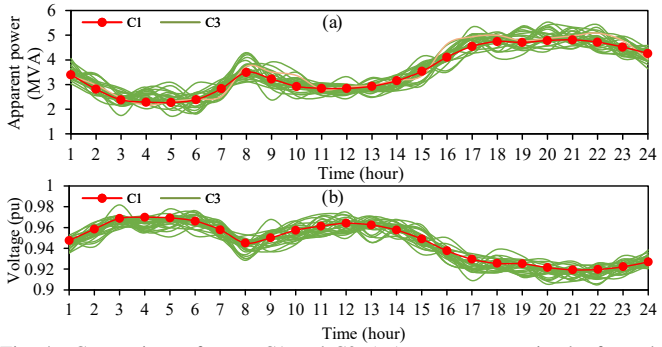

Fig. 4. Comparison of cases C1 and C3 a) Apparent power intake from the upper grid b) Minimum voltage in the system.

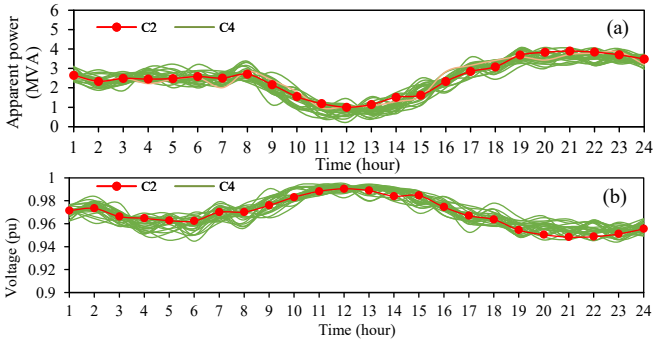

Fig. 5. Comparison of cases C2 and C4 a) Apparent power intake from the upper grid b) Minimum voltage in the system.

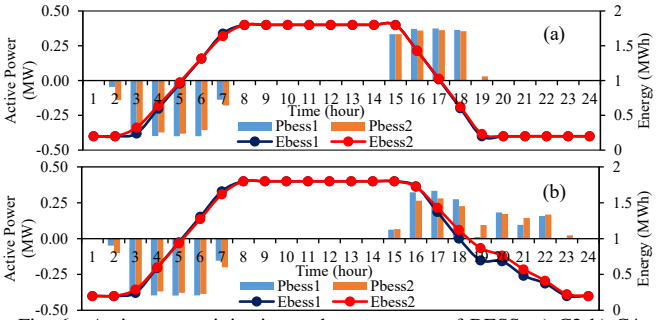

Fig. 6. Active power injection and energy state of BESS: a) C2 b) C4.

reactive power injection from the SCB and BESS into the grid is plotted in Fig. 7(a) and Fig. 7(c), respectively.

Case-3 (C3): The uncertainty from the PV, WT, and load is considered in this case. It is a comprehensive study of Case-1 with uncertainty inclusion. Parameters related to the beta distribution function are estimated using the expressions discussed in Section III. The standard deviation of the load is assumed as 5%. A 10,000 number of random scenarios are constructed using the MCS technique and reduced to 25 scenarios using the Kantorovich probability distance method. C3 is the simple one without BESS and SCB. Fig.4 depicts the related apparent power intake and minimum voltage in the system for all scenarios.

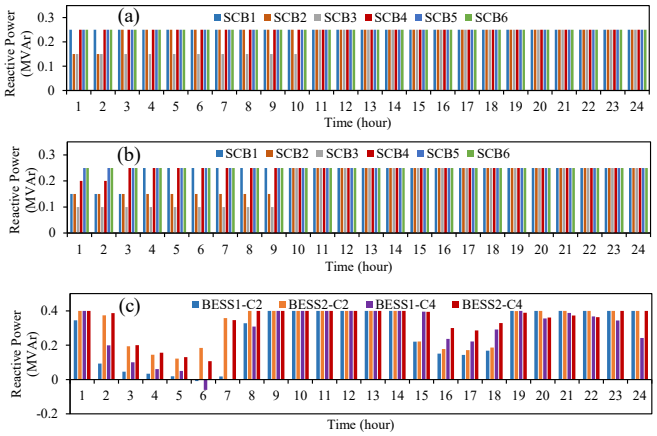

Fig. 7. a) Reactive power participation from SCB in C2 b) Reactive power participation from SCB in C4 c) Reactive power participation from BESS.

Case-4 (C4): It represents the stochastic optimal scheduling of ADN coupled with BESS and SCB. It is an extended study of Case-2 with uncertainty inclusion. The apparent power intake and minimum voltage in the system are displayed in Fig. 5. The optimal charge/discharge power and energy state of both BESSs are displayed in Fig. 6(b). The reactive power injection from the BESS and SCB are displayed in Fig. 7(c) and Fig. 7(b) respectively. Similar to Case-2, both BESSs are charging, when grid price is low and discharging, when grid price is high, but there will be a slight change in charge/discharge power magnitude due to the stochastic nature of load and renewable generation.

Table III presents the comparison of results from different cases. From this table, it is observed that the daily operational cost is reduced from \$5528.20 (C1) to \$4902.33 (C2). This results in a saving of \$625.87 in daily operational cost. The daily active and reactive energy losses are reduced in C2 by 1.3115 MWh and 0.856 MVArh, respectively, as compared to C1. In C2, the peak demand on substation over a day is significantly reduced to 3.8906 MVA from 4.8078 MVA in C1. This reduction in the peak demand on substation eliminates the requirement of strengthening of substation transformer. Further, in C2, the minimum voltage in the system is significantly improved to 0.9483 pu from 0.9193 pu in C1. In C4, the expected daily operational cost is reduced to \$4785.28 from \$5585.72 (C3) due to active and reactive power participation from BESS and SCB. The expected daily active and reactive energy losses are saved by 1.498 MWh and 0.9369 MVArh, respectively, in C4 in comparison to C3. Further, the peak demand in the system is reduced to 4.0775 MVA (C4) from 5.5256 MVA (C3). In C4, a significant improvement in the minimum voltage in the system is also observed. Therefore, the proposed formulation is able to improve the overall performance of ADN.

TABLE III
COMPARISON OF DIFFERENT CASES

Parameter	C1	C2	C3	C4
Operational cost (\$)	5528.20	4902.33	5585.72	4785.28
Active energy losses (MWh)	2.8410	1.5295	2.9463	1.4483
Reactive energy losses (MVArh)	1.8890	1.0330	1.9559	1.0190
Peak demand (MVA)	4.8078	3.8906	5.5256	4.0775
Minimum voltage (pu)	0.9193	0.9483	0.9048	0.9441

IV. CONCLUSION

A two-stage stochastic day-ahead scheduling for an ADN coupled with BESS and SCB is framed as a MISOCP model. By optimally setting the hourly dispatches for BESS and SCB, it has been observed that the operational costs have been saved by \$625.87 and \$800.44 in both deterministic and stochastic programming, respectively. Similarly, the active reactive energy losses and peak demand in the network over a day have significantly reduced with the active and reactive power participation by BESS and SCB. A notable improvement in the voltage profile with the optimal dispatch of BESS and SCB is observed. So, the results certify that optimal day-ahead scheduling of BESS and SCB can significantly improve various performance indices of the ADN.

REFERENCES

[1] Mongird, K., Viswanathan, V. V., Balducci, P. J., Alam, M. J. E., Fotedar, V., Koritarov, V. S., Hadjerioua, B. (2019). Energy storage technology and cost characterization report (No. PNNL-28866). Pacific Northwest National Lab.(PNNL), Richland, WA (United States), 2019.

[2] I. C. da Silva, S. Carneiro, E. J. de Oliveira, J. de Souza Costa, J. L. R. Pereira and P. A. N. Garcia, "A Heuristic Constructive Algorithm for Capacitor Placement on Distribution Systems," in *IEEE Transactions on Power Systems*, vol. 23, no. 4, pp. 1619-1626, Nov. 2008.

[3] A. Gabash and P. Li, "Active-Reactive Optimal Power Flow in Distribution Networks With Embedded Generation and Battery Storage," in *IEEE Transactions on Power Systems*, vol. 27, no. 4, pp. 2026-2035, Nov. 2012.

[4] Abapour, Saeed, Sayyad Nojavan, and Mehdi Abapour. "Multi-objective short-term scheduling of active distribution networks for benefit maximization of DisCos and DG owners considering demand response programs and energy storage system." *Journal of Modern Power Systems and Clean Energy*, 6.1: 95-106, 2018.

[5] Jha, B.K., Singh, A., Kumar, A., Dheer, D.K., Singh, D. and Misra, R.K. Day ahead scheduling of PHEVs and D-BESSs in the presence of DGs in the distribution system. *IET Electrical Systems in Transportation*, 10(2), pp.170-184, 2019.

[6] Helal, S.A., Ahmed, M.H., Salama, M.M. and Shaaban, M.F., 2018, May. Optimal Scheduling of Battery Energy Storage Systems in Unbalanced Distribution Networks. in *IEEE Canadian Conference on Electrical & Computer Engineering (CCECE)* (pp. 1-4), 2018.

[7] Montoya, Oscar Danilo, and Walter Gil-González. "Dynamic active and reactive power compensation in distribution networks with batteries: A day-ahead economic dispatch approach." *Computers & Electrical Engineering*, 85, 106710, 2020.

[8] D. O. Sidea, I. I. Picioroaga and C. Bulac, "Optimal Battery Energy Storage System Scheduling Based on Mutation-Improved Grey Wolf Optimizer Using GPU-Accelerated Load Flow in Active Distribution Networks," in *IEEE Access*, vol. 9, pp. 13922-13937, 2021.

[9] J. Arkhangelski, M. Abdou-Tankari and G. Lefebvre, "Day-Ahead Optimal Power Flow for Efficient Energy Management of Urban Microgrid," in *IEEE Transactions on Industry Applications*, vol. 57, no. 2, pp. 1285-1293, March-April 2021.

[10] L. H. Macedo, J. F. Franco, M. J. Rider and R. Romero, "Optimal Operation of Distribution Networks Considering Energy Storage Devices," in *IEEE Transactions on Smart Grid*, vol. 6, no. 6, pp. 2825-2836, Nov. 2015.

[11] R. Zafar, J. Ravishankar, J. E. Fletcher and H. R. Pota, "Optimal Dispatch of Battery Energy Storage System Using Convex Relaxations in Unbalanced Distribution Grids," in *IEEE Transactions on Industrial Informatics*, vol. 16, no. 1, pp. 97-108, Jan. 2020.

[12] Y. Xu, Z. Y. Dong, R. Zhang and D. J. Hill, "Multi-Timescale Coordinated Voltage/Var Control of High Renewable-Penetrated Distribution Systems," in *IEEE Transactions on Power Systems*, vol. 32, no. 6, pp. 4398-4408, Nov. 2017.

[13] Conejo, Antonio J., Miguel Carrión, and Juan M. Morales. Decision making under uncertainty in electricity markets. Vol. 1. New York: Springer, 2010.

[14] R. A. Jabr, "Radial distribution load flow using conic programming," in *IEEE Transactions on Power Systems*, vol. 21, no. 3, pp. 1458-1459, Aug. 2006.

[15] M. Farivar and S. H. Low, "Branch Flow Model: Relaxations and Convexification—Part I," in *IEEE Transactions on Power Systems*, vol. 28, no. 3, pp. 2554-2564, Aug. 2013.

[16] S. Golshannavaz, S. Afsharnia and F. Aminifar, "Smart Distribution Grid: Optimal Day-Ahead Scheduling With Reconfigurable Topology," in IEEE Transactions on Smart Grid, vol. 5, no. 5, pp. 2402-2411, Sept. 2014.

[17] Web application-renewable ninja. Output of Photovoltaic and Wind power. Available: https://www.renewables.ninja.